ARTICLE

Dinuclear Ligand-to-Ligand Charge Transfer Complexes

David A. Shultz,*[a] Riley Stephenson[a]† and Martin L. Kirk *[b-d]

Received 00th January 20xx,
Accepted 00th January 20xx

DOI: 10.1039/x0xx00000x

The synthesis and characterization of dinuclear ligand-to-ligand charge transfer complexes are described. Each complex is comprised of square-planar platinum(II) coordinated to a 3-*tert*-butyl-orthocatecholate donor and a 4,4'-di-*tert*-butyl-2,2'-bipyridine acceptor. Both complexes exhibit donor → acceptor ligand-to-ligand charge transfer (LL'CT) bands in the visible spectrum. The platinum complexes are covalently attached at the catecholate 5-position to either a *meta*- or *para*-phenylene bridge fragment. Both cyclic voltammetry and electronic absorption spectroscopy exhibit features characteristic of intramolecular interaction between the platinum centres. The LL'CT excited state lifetimes are ~twofold longer than the mononuclear parent complex. The properties of these complexes are discussed and compared to similar complexes in the literature.

Introduction

Complexes of group 10 d^8 metal ions that possess diimine acceptor ligands and dichalcogenolene donor ligands (*e.g.*, dithiolate and catecholate, Fig. 1) have been studied for decades due to their luminescent properties and for solar energy conversion,[1-9] but have gained recent attention due to their use in understanding vibronic activation of non-radiative decay processes (*e.g.* spin-vibronic coupling).[10, 11] A characteristic feature of this class of compounds is a dipole-allowed ($\varepsilon_{LL'CT} \approx$ 4-6000 $M^{-1}\bullet cm^{-1}$) dichalcogenolene → diimine ligand-to-ligand charge transfer (LL'CT) band in the visible to NIR region of the electronic absorption spectrum (≈ 600 nm – 1100 nm).[12] The nature of this LL'CT transition is best described as a one-electron promotion from the donor-dominated HOMO to the acceptor-dominated LUMO that leads to a high degree of charge separation in the LL'CT excited state.[10-14] The HOMO-LUMO orbital overlap is mediated by the Pt^{2+} ion and is achieved by a modest (≈ 5%) metal-acceptor contribution to the HOMO, and corresponding metal-donor contribution to the LUMO[10]. Heavy chalcogen (Figure 1; E = O, S, Se, E' = S, Se) donor atom substitutions provide a key mechanism for intersystem crossing (ISC) to photoluminescent triplet states ($S_1 \rightarrow T_2 \rightarrow T_1$: $\phi_{PL} \approx$ 10%). This occurs by lowering the energy of the T_2 state relative to S_1 (Figure 1).[11] In cases where E ≠ E', photoluminescent emission

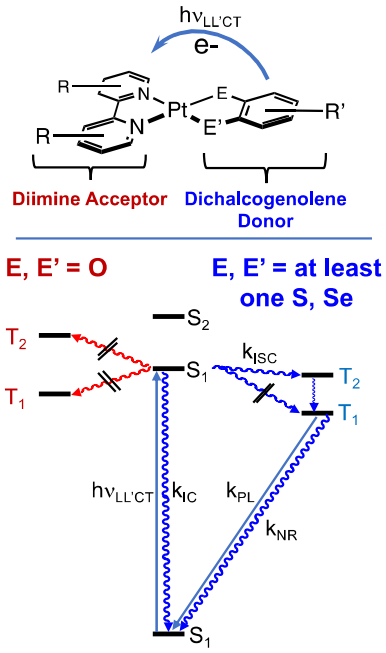

Figure 1. ***Left:*** Molecular structure of LL'CT complexes. Metal ion may also be Ni(II) or Pd(II). ***Right:*** Jablonski diagrams.

from the T_1 triplet state to the S_1 ground state is enabled by static distortions that derive from T_1-T_2 vibronic coupling.[10, 11] However, when the donor is a catecholate (*e.g.* E = E' = O) intersystem crossing in this C_{2v} chromophore is symmetry forbidden, and the excited S_1 singlet decays by fast and efficient non-radiative internal conversion (IC) on a ~10^2 ps time scale.[10, 11]

More recently, complexes of this type have been designed that possess radical-appended catecholate donors (*e.g.* R' contains a stable nitronyl nitroxide (NN) radical that is covalently attached to a the catecholate via a bridge fragment

[a] *Department of Chemistry, North Carolina State University, Raleigh, North Carolina 27695-8204, United States.*
[b] *Department of Chemistry and Chemical Biology, The University of New Mexico, MSC03 2060, 1 University of New Mexico, Albuquerque, NM 87131-0001.*
[c] *The Center for High Technology Materials, The University of New Mexico, Albuquerque, New Mexico 87106, United States.*
[d] *Center for Quantum Information and Control (CQuIC), The University of New Mexico, Albuquerque, New Mexico 87131-0001, United States.*
† Current address: Department of Chemistry, Duke University, Durham, NC 27708, United States.
Electronic Supplementary Information (ESI) available: [details of any supplementary information available should be included here]. See DOI: 10.1039/x0xx00000x

(B), (**bpy)Pt(CAT-B-NN)** Figs. 1 and 2). These radical-elaborated LL'CT systems exhibit controllable photoinduced ground state electron spin polarization (ESP)[15-18], relevant to quantum information science applications, that is detected by transient electron paramagnetic resonance (TREPR) spectroscopy.[19] The proposed mechanism for the generation of ground state ESP involves fast excited state trip-doublet – trip-quartet ($^2T_1 - {}^4T_1$) mixing that results in a non-Boltzmann populations of the m_s-level populations in the $^2T_1$ state prior to non-radiative decay to the doublet ground state ($^2S_0$). The corresponding non-Boltzmann population of the ground state is observed to be either enhanced absorptive[15, 16, 18] or enhancemissive[17] as monitored in the TREPR response signal. Distinguishing features if these radical-elaborated chromophores with respect to QIS applications include localized radical excited state contributions to the ESP, and a large time difference between photocycle initiation of the spin polarized ground state (~ns regime) and the lifetime (ms regime) of the spin-polarized EPR signal that corresponds to the longitudinal relaxation time (T_1) of the appended nitronyl nitroxide radical.

The LL'CT excited state lifetimes of the **(bpy)Pt(CAT-B-NN)** complexes exhibit a power-law relationship with the excited state exchange parameter that determines the trip-doublet – trip-quartet energy gap.[20] Notably, the magnitude of the ESP of these complexes also exhibits a power-law dependence with the same excited state exchange parameter.[15] Thus, there may be a connection between the LL'CT excited state lifetime and the magnitude of the observed ESP. Such a relationship would define the timescale of the trip-doublet – trip-quartet equilibrium required for polarization of the m_s levels.

Therefore, we are interested in exploring a potential relationship between the magnitude and sign of the ground state ESP, and the lifetime of the LL'CT excited state in structurally diverse radical-elaborated donor-acceptor chromophores. Herein, we describe our initial efforts at probing lifetime-ESP relationships this area by studying the effects on excited state lifetime of covalently linking *two* LL'CT chromophores to a common bridging unit ((***m*-Ph[(CAT)Pt(bpy)]$_2$** and ***p*-Ph[(CAT)Pt(bpy)]$_2$**)) in the absence of a stable radical moiety, Fig. 2.

Results

Synthesis. Dinuclear Pt(II) complexes were prepared using bis(catechol)s that were synthesized according to Scheme 1. Palladium-catalyzed coupling of boronic ester **1**[21] and either 1,3-

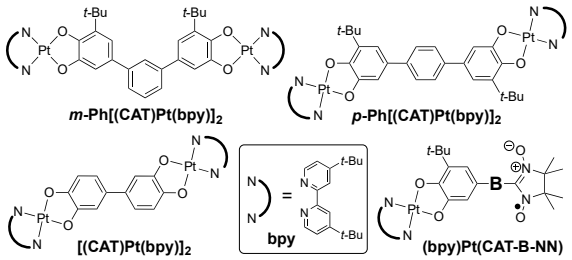

Figure 2. *Top:* Complexes in this study (***m*-Ph[(CAT)Pt(bpy)]$_2$** and ***p*-Ph[(CAT)Pt(bpy)]$_2$**). *Bottom, Left:* a previously reported dinuclear complex, **[(CAT)Pt(bpy)]$_2$**. *Bottom, Right:* previously reported nitronyl-nitroxide mononuclear complexes, **(bpy)Pt(CAT-B-NN)**.

diiodobenzene (**2**) or 1,4-diiodobenzene (**3**) produced the methoxymethyl- (MOM) protected bis-chelating ligands, ***m*-Ph[CAT(MOM)$_2$)]$_2$** and ***p*-Ph[CAT(MOM)$_2$)]$_2$**. Standard conditions were used to deprotect and then coordinate[20, 22] these bis(catechol)s to bis(4,4'-di-*tert*-butyl)-2,2'-bipyridine dichloride, bpyPtCl$_2$, to yield dark purple colored solids after purification by chromatography.

Electronic Absorption Spectroscopy. The solution electronic absorption spectra for ***m*-Ph[(CAT)Pt(bpy)]$_2$** and ***p*-Ph[(CAT)Pt(bpy)]$_2$** were collected at room temperature in methylene chloride and are shown in Fig. 3. The characteristic LL'CT absorption bands appear at ca 600 nm (16,700 cm^{-1}), and the molar extinction coefficients are approximately twice as large as that of the mononuclear complex, **(3,5-di-*t*-Bu)$_2$CAT)Pt(bpy)**.[11, 23] We observe a slight bathochromic- and hyperchromic shift of the LL'CT band of ***p*-Ph[(CAT)Pt(bpy)]$_2$** compared to ***m*-Ph[(CAT)Pt(bpy)]$_2$**. Due to the modest transition dipole and distance between the two LL'CT chromophores, no exciton splitting[24] is observed in the dimeric complexes. However, an appreciable shift to higher energy of the UV band is observed in the order **(3,5-di-*t*-Bu)$_2$CAT)Pt(bpy)** > ***m*-Ph[(CAT)Pt(bpy)]$_2$** > ***p*-Ph[(CAT)Pt(bpy)]$_2$**, which parallels the expected delocalization of the CAT onto the Ph ring in ***m*-Ph[(CAT)Pt(bpy)]$_2$**, and onto the other half of the dimer in ***p*-Ph[(CAT)Pt(bpy)]$_2$**. This interpretation mirrors the results of electrochemical experiments on these complexes, *vide infra*.

Electrochemistry. Cyclic voltammograms (CVs) and differential pulse voltammograms (DPVs) of ***m*-Ph[(CAT)Pt(bpy)]$_2$** and ***p*-Ph[(CAT)Pt(bpy)]$_2$** are shown in Fig. 4, and both complexes exhibit semiquinone-catecholate- (SQ/CAT; ~+100 mV vs. ferrocene/ferrocenium) as well as bpy-bpy$^{-\bullet}$ (~-1800 mV vs. ferrocene/ferrocenium) redox couples.

Scheme 1. Synthesis of ***m*-Ph[(CAT)Pt(bpy)]$_2$** and ***p*-Ph[(CAT)Pt(bpy)]$_2$**.

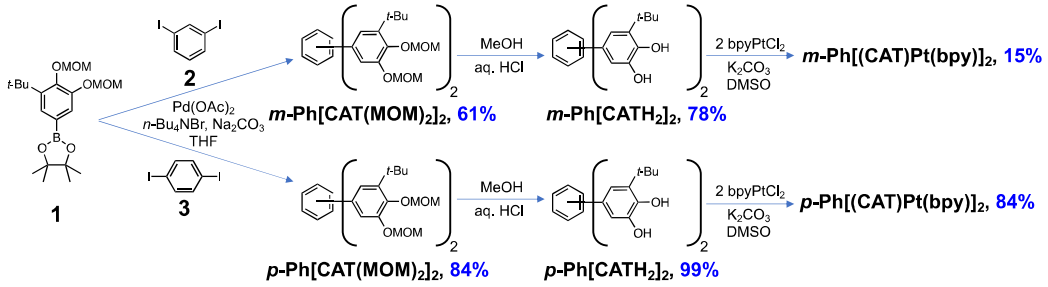

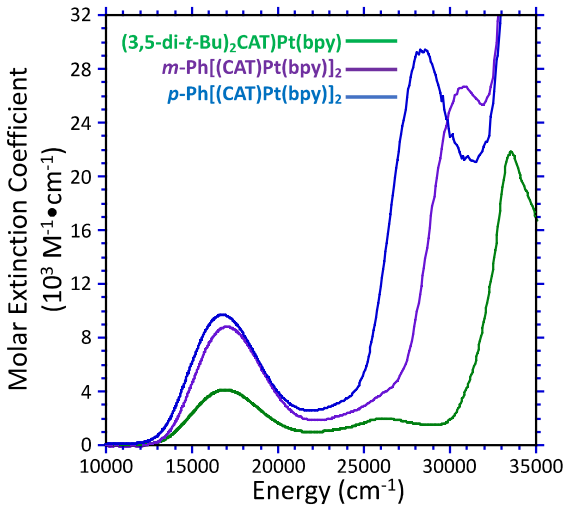

Figure 3. Electronic absorption spectra of dinuclear- and mononuclear complexes as solutions in methylene chloride.

The redox splitting of the two dioxolene redox couples is greater for ***p*-Ph[(CAT)Pt(bpy)]$_2$** (130 mV; conjugated CAT moieties) than for ***m*-Ph[(CAT)Pt(bpy)]$_2$** (95 mV; cross-conjugated CAT moieties) as expected, but less than that for a previously reported bis(CAT) complex in which the two CAT moieties are directly bonded (Fig. 2 right, 340 mV).[23, 25] The through space and through bond distances are too great for the expected small redox splitting of the bpy↔bpy$^{-\bullet}$ couples to be observed, and these appear as two, isopotential one-electron processes.

Ultrafast Transient Absorption Spectroscopy. Room temperature transient absorption spectra were recorded in CH_2Cl_2 under a argon atmosphere using 640 nm, ~80 fs pump pulses. These resultant transient absorption data are displayed as 2D contour plots (in linear space out to 10 ps delay times) and as difference spectra across a series of delay times. These data are shown collectively in Fig. 5. The data for **(3,5-di-*t*-Bu)$_2$CAT)Pt(bpy)**, ***m*-Ph[(CAT)Pt(bpy)]$_2$**, and ***p*-Ph[(CAT)Pt(bpy)]$_2$** are typical of this type of CAT → bpy LL'CT chromophore, and are characterized by a bleach of the LL'CT bands near 600 nm and excited state absorption features that span the 400-600 nm (bpy$^{-\bullet}$ and semiquinone) and 650-800 nm (semiquinone) ranges.[23] Global fit analyses were performed using a sequential biexponential decay model, and the best fits of the model to the data reveal both short- (τ_{VR} = 1.07 ± 0.10 ps, ***m*-Ph[(CAT)Pt(bpy)]$_2$**; τ_{VR} = 1.06 ± 0.07 ps, ***p*-Ph[(CAT)Pt(bpy)]$_2$**) and long ($\tau_{LL'CT}$ = 1180 ± 340 ps, ***m*-Ph[(CAT)Pt(bpy)]$_2$**; $\tau_{LL'CT}$ = 1040 ± 250 ps, ***p*-Ph[(CAT)Pt(bpy)]$_2$**) timescale components. We assign the faster component to vibrational cooling (τ_{VR}) and the longer component to non-radiative $S_1 \rightarrow S_0$ internal conversion ($\tau_{LL'CT}$) analogous to what has been previously observed in mononuclear complexes.[20, 23]

Discussion

The electronic absorption spectra of ***m*-Ph[(CAT)Pt(bpy)]$_2$** and ***p*-Ph[(CAT)Pt(bpy)]$_2$** lack exciton splitting[26, 27] of the LL'CT bands, and this can be explained by the weak electronic coupling of the chromophores in the dimer molecules. This result is anticipated due to the relatively weak oscillator strength of the LL'CT bands, and the fact that ***p*-Ph[(CAT)Pt(bpy)]$_2$** has the LL'CT transition dipoles are oriented in opposite directions. Redox splitting of the CAT/SQ couples is observed in both CV and DPV, and the magnitude is consistent with the nature of the linkage mediated by *meta*- and *para*-

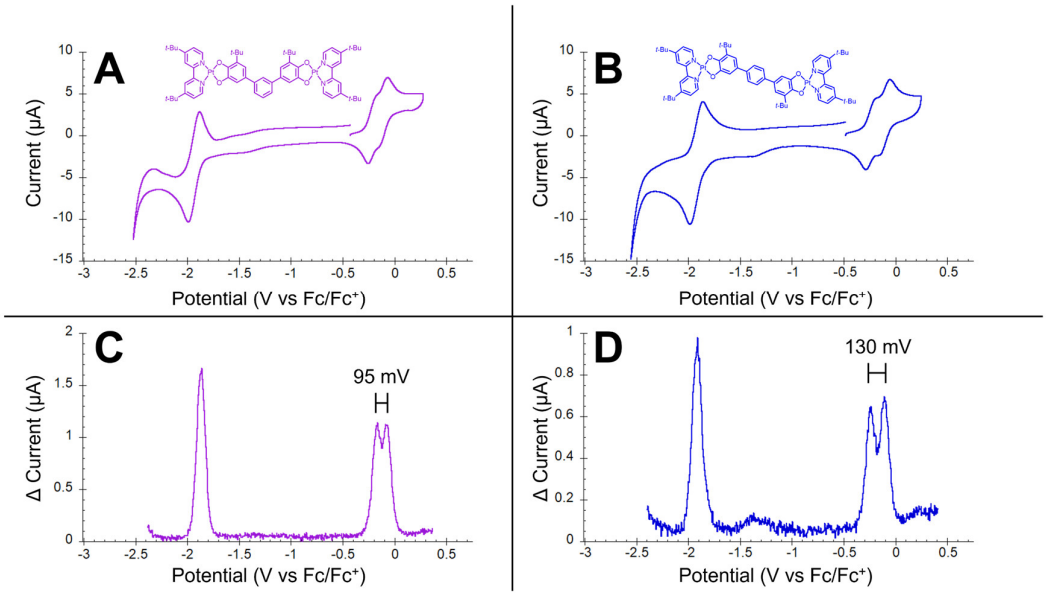

Figure. 4. Top: Cyclic voltammograms of ***m*-Ph[(CAT)Pt(bpy)]$_2$** (**A**) and ***p*-Ph[(CAT)Pt(bpy)]$_2$** (**B**). Bottom: Differential pulse voltammograms of ***m*-Ph[(CAT)Pt(bpy)]$_2$** (**C**) and ***p*-Ph[(CAT)Pt(bpy)]$_2$** (**D**). Potentials are in volts vs. Fc/Fc$^+$. Note redox splitting of CAT↔SQ couple. No redox splitting of bpy↔bpy-• is observed. We assign the wave at -1.4 V to a small electroactive impurity.

phenylene bridges.[26] The modest redox splitting precludes isolating the mixed valent forms. Since the LL'CT transition (HOMO → LUMO) shows very little change in transition energy across the series, the HOMO-LUMO gap must not vary appreciably upon incorporation of the bridge fragment.

Table 1. LL'CT Excited State Lifetimes[a] of Platinum Complexes

Complex	$\tau_{LL'CT}$ (ps)	Reference
(bpy)Pt(3,5-*t*-Bu$_2$CAT)	630 ± 12[b]	23
***m*-Ph[(CAT)Pt(bpy)]$_2$**	1180 ± 340	*This work*
***p*-Ph[(CAT)Pt(bpy)]$_2$**	1040 ± 250	*This work*
[(CAT)Pt(bpy)]$_2$	690 ± 15[b]	23
(bpy)Pt(CAT-NN)	250 ± 30	21
(bpy)Pt(CAT-Th-NN)[c]	410 ± 80	21
(bpy)Pt(CAT-*p*-Ph-NN)	640 ± 30	21
(bpy)Pt(CAT-*m*-Ph-NN)	790 ± 20	21
(bpy)Pt(CAT-Ph$_2$-NN)[d]	1010 ± 30	21

[a]Lifetimes from transient absorption spectroscopy at room temperature. [b]Lifetime from transient IR spectroscopy. [c]**Th** = 2,5-thiophenyl. [d]**Ph$_2$** = 4,4'-biphenyl.

Ph[(CAT)Pt(bpy)]$_2$ LL'CT chromophores are covalently attached via *meta*- and *para*- connectivity, respectively, to a phenylene bridge. Bardeen and Martinez reported that donor and acceptor moieties separated by 1,3-diethynyl-*meta*-phenylene undergo charge recombination decay rates that are orders of magnitude *slower* than the same donor-acceptor dyad separated by 1,3-diethynyl-*meta*-phenylene.[28] In the present case detailed here, the *meta*- and *para*-phenylene bridges connect a *pair* of donor-acceptor dyads. Consequently, the relaxation pathway(s) do not rely exclusively on electronic coupling *through*, or mediated by, the phenylene bridge. $S_1 \rightarrow S_0$ non-radiative decay within a monomer fragment involves deexcitation from the LUMO to the HOMO. Given that the HOMO-LUMO gap across this series is nearly invariant, as determined by electronic absorption spectroscopy, the LL'CT excited state lifetimes for ***m*-Ph[(CAT)Pt(bpy)]$_2$** and ***p*-Ph[(CAT)Pt(bpy)]$_2$** are also nearly equivalent and are independent of the bridge fragment.

Ultrafast transient absorption spectroscopy has been used to determine the LL'CT excited state lifetimes (Fig. 5) for ***m*-Ph[(CAT)Pt(bpy)]$_2$** and ***p*-Ph[(CAT)Pt(bpy)]$_2$**. These data were fit

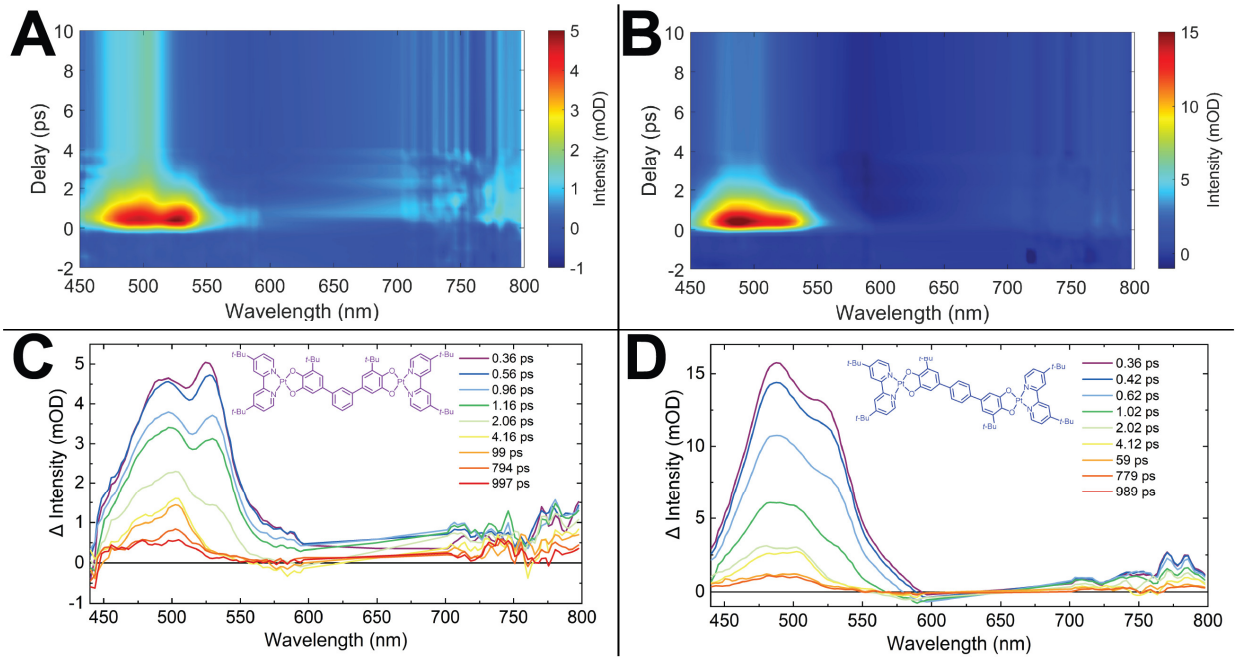

Figure. 5. Ultrafast transient absorption spectra for ***m*-Ph[(CAT)Pt(bpy)]$_2$** (**A** and **C**) and ***p*-Ph[(CAT)Pt(bpy)]$_2$** (**B** and **D**).

Ligand-to-ligand charge transfer complexes comprised of catecholate donors are characterized by subnanosecond excited singlet lifetimes that relax solely by spin allowed $S_1 \rightarrow S_0$ non-radiative decay. Weinstein and coworkers reported that dimeric **[(CAT)Pt(bpy)]$_2$**, where the two chromophores are directly connected without a bridge, also decays non-radiatively with a lifetime that is nearly identical to that of the mononuclear complex, **(3,5-*t*-Bu$_2$CAT)Pt(bpy)**.[23] We were intrigued by this result, and wished to further explore the key factors that affect the LL'CT lifetimes of bridged dimeric complexes. The dinuclear ***m*-Ph[(CAT)Pt(bpy)]$_2$** and ***p*-Ph[(CAT)Pt(bpy)]$_2$** to two exponential decay functions yielding τ_{VR} and $\tau_{LL'CT}$ lifetimes. We tentatively assign the shorter lifetime, τ_{VR}, to either a vibrational relaxation process, or to conformational relaxation (*i.e.* rotations about CAT-phenylene bonds). Two peaks observed at ~487 nm and ~ 525 nm, which are separated by ~ 1,500 cm^{-1}, provide support for two conformers being present at short timescales. Rapid relaxation (~ 1 ps) to a more stable conformer is revealed by the observation of two peaks in the 480 nm region that are observed from 1-100 ps for ***m*-Ph[(CAT)Pt(bpy)]$_2$** (Fig. 5C) and from 1-60 ps for ***p*-Ph[(CAT)Pt(bpy)]$_2$** (Fig. 5D). The longer lifetimes, $\tau_{LL'CT}$,

corresponds to the lifetime of the LL'CT excited state. The LL'CT lifetimes that we observe here are ~2-fold *longer* than that observed for monomeric **(3,5-*t*-Bu$_2$CAT)Pt(bpy)** (Table 1).[23] These results are surprising given the additional single bonds, which facilitate nonradiative decay via the "loose bolt effect"[29], of the bis(catecholate) bridging ligands relative to the dinuclear complex studied by Weinstein and coworkers.[23] Thus, we suggest that excited state stabilization via electron delocalization onto the second CAT moiety may contribute to the modest increase in excited state lifetimes, and future efforts will explore this possibility.

Conclusions

Two dinuclear LL'CT complexes comprised of catecholate donors and bipyridine acceptors, ***m*-Ph[(CAT)Pt(bpy)]$_2$** and ***p*-Ph[(CAT)Pt(bpy)]$_2$**, were prepared and characterized. Electronic absorption spectroscopy indicates only slight changes in the $S_0 \rightarrow S_1$ LL'CT transition energy across this series of molecules. Thus, while there may be some differential delocalization of the oxidized CAT (*e.g.* SQ) hole via the *meta*- and *para*-phenylene bridges, this does not appear to affect the $S_0 \rightarrow S_1$ transition energy, which is dominated by a CAT(HOMO) → bpy(LUMO) one-electron promotion contribution. The localized nature of the LUMO, which is occupied in the LL'CT excited state (CAT+•/bpy-• charge separated state), prevents true mixed-valent characteristics of these and related[23] complexes. We have also used transient absorption spectroscopy to probe the LL'CT excited state formation and decay in these dinuclear complexes. While the lifetime of ***m*-Ph[(CAT)Pt(bpy)]$_2$** was slightly longer than that of ***p*-Ph[(CAT)Pt(bpy)]$_2$**, both decayed ~2-fold slower than the parent mononuclear complex, **(3,5-*t*-Bu$_2$CAT)Pt(bpy)** and the previously reported dinuclear complex, **[(CAT)Pt(bpy)]$_2$**. This behavior may be explained by excited state delocalization mediated by both *meta*- and *para*-phenylene bridges. Collectively, these results show that dinuclear complexes comprised of phenylene-bridged LL'CT chromophores have excited state lifetimes that are not attenuated by additional vibrational modes resulting from elaborated bridge units. Such structure-property relationships are crucial to probing effects of excited state lifetimes on the magnitude and/or sign of photoinduced electron spin polarization.[15-18]

Experimental

General

See supporting information for general considerations and characterization data and spectra.

Synthesis

3,3''-Di-*tert*-Butyl-4,4'',5,5''-*tetrakis*(methoxymethoxy)-1,1':3',1''-terphenyl (***m*-Ph[(CAT(MOM)$_2$]$_2$**). 2-(3-(*tert*-Butyl)-4,5-bis(methoxymethoxy)phenyl)-4,4,5,5-tetramethyl-1,3,2-dioxaborolane (**1**) (502 mg, 1.32mmol), 1,3-diiodobenzene (**2**, 218 mg, 0.661 mmol), sodium carbonate (279 mg, 2.63 mmol), tetrabutylammonium bromide (45 mg, 0.14 mmol), and palladium(II) acetate (4 mol%) was placed into a Schlenk flask and purged with argon. Then, degassed tetrahydrofuran (60 mL) and degassed water (20 mL) was added to the reaction flask. This solution was then stirred at 50°C for 22h. Then, the reaction was washed with a saturated sodium chloride solution and the product was extracted with ethyl acetate. The organic layer was then dried and concentrated resulting in a red solid. This solid was purified on a silica column with a gradient eluent system (first pure hexanes was used to remove remaining 1,3-diiodobenzene, then ethyl acetate was used to elute the product). The condensed fractions containing the product yielded 233 mg of a yellow oil (61% yield).

5,5''-Di-*tert*-butyl-[1,1':3',1''-terphenyl]-3,3'',4,4''-tetraol ((***m*-Ph[(CATH$_2$]$_2$**). ***m*-Ph[(CAT(MOM)$_2$]$_2$** (105 mg, 0.180 mmol) was placed in a round bottom flask and purge pumped three times on a Schlenk line with nitrogen gas. Then, degassed methanol (9mL) and 12M aqueous hydrochloric acid (1 mL) were added to the reaction mixture. This solution was stirred at room temperature under a positive pressure of nitrogen gas for 22 h. Then the reaction was dripped into a separatory funnel, washed with an aqueous solution of saturated sodium chloride, and the product was extracted with ethyl acetate. The organic layer was concentrated and placed under vacuum to dry. This yielded 57 mg of oily solid (78% yield). ^{1}H NMR (600 MHz, DMSO-d_6) δ 9.54 (s, 2H), 8.19 (s, 2H), 7.51 (s, 1H), 7.42 (dd, *J* = 8.7, 6.3 Hz, 1H), 7.40 – 7.36 (m, 2H), 6.97 (d, *J* = 2.1 Hz, 2H), 6.93 (d, *J* = 2.1 Hz, 2H), 1.40 (s, 18H). ^{13}C NMR (101 MHz, DMSO-d_6) δ 145.45, 143.96, 141.75, 135.94, 130.37, 129.26, 124.22, 123.85, 115.65, 111.35, 34.47, 29.44. HRMS (ESI) m/z: [M-H]$^-$ Calcd for $C_{26}H_{30}O_4$ 405.20713; Found 405.20587.

3,3''-Di-*tert*-butyl-4,4'',5,5''-tetrakis(methoxymethoxy)-1,1':4',1''-terphenyl (***p*-Ph[(CAT(MOM)$_2$]$_2$**). 2-(3-(*tert*-Butyl)-4,5-bis(methoxymethoxy)phenyl)-4,4,5,5-tetramethyl-1,3,2-dioxaborolane (**1**) (250 mg, 0.66 mmol), 1,4-diiodobenzene (109 mg, 0.329 mmol), sodium carbonate (141 mg, 1.33 mmol), tetra-*n*-butylammonium bromide (23 mg, 0.072 mmol), and palladium(II) acetate (4.5 mg, 0.02 mmol) was placed into a Schlenk flask and purged with argon. Then, degassed tetrahydrofuran (45 mL) and degassed water (15mL) was added to the reaction flask. This solution was then stirred at 50°C for 46h. Then, the reaction was washed with a saturated sodium chloride solution and the product was extracted with ethyl acetate. The organic layer was then dried and concentrated resulting in a red solid. This solid was purified on a silica column with a gradient eluent system (first pure hexanes was used to remove remaining 1,4-diiodobenzene, then ethyl acetate was used to elute the product). The condensed fractions containing the product yielded 160 mg of yellow oil (84% yield). ^{1}H NMR (400 MHz, chloroform-*d*) δ 7.59 (s, 4H), 7.29 (d, *J* = 2.1 Hz, 2H), 7.26 (d, *J* = 2.1 Hz, 2H), 5.25 (s, 4H), 5.24 (s, 4H), 3.68 (s, 6H), 3.54 (s, 6H), 1.47 (s, 18H). HRMS (ESI) m/z: [M+Na]$^+$ Calcd for $C_{34}H_{46}O_8$ 605.30849; Found 605.30848.

5,5''-Di-*tert*-butyl-[1,1':4',1''-terphenyl]-3,3'',4,4''-tetraol (***p*-Ph[(CATH$_2$]$_2$**). ***p*-Ph[(CAT(MOM)$_2$]$_2$** (102 mg, 0.175 mmol) was placed in a round bottom flask and purge pumped three times on a Schlenk line with nitrogen gas. Then, degassed methanol (9 mL) and 12M aqueous hydrochloric acid (1mL) were added to the reaction mixture. This solution was stirred at room temperature under a positive pressure of nitrogen gas for 2

days. Then the reaction was dripped into a separatory funnel, washed with an aqueous solution of saturated sodium chloride, and the product was extracted with ethyl acetate. The organic layer was concentrated and placed under vacuum to dry. This yielded 70 mg of oily solid (99% yield). ^{1}H NMR (400 MHz, DMSO-d_6) δ 9.52 (s, 2H), 8.16 (s, 2H), 7.52 (s, 4H), 6.97 (s, 2H), 6.93 (s, 2H), 1.39 (s, 18H).

p*-Ph[(CAT)Pt(bpy)]$_2$.** (p*-Ph[(CATH$_2$]$_2$** (51 mg, 0.13 mmol), 4,4'-di-*tert*-butyl-2,2'-dipyridyl platinum dichloride (bpyPtCl$_2$)[30] (132mg, 0.247mmol), and potassium carbonate (71mg, 0.52 mmol) were placed in an oven-dried Schlenk flask and purged/pumped three times on a Schlenk line with nitrogen. Then degassed dimethyl sulfoxide (4mL) was added to the reaction. The reaction was then stirred under a positive pressure of nitrogen at room temperature for 45h. The resulting dark purple solution was then dripped into a stirring solution of saturated sodium chloride (200mL) resulting in the precipitation of a dark a purple solid. This precipitate was collected via vacuum filtration and dissolved in ethyl acetate and dichloromethane. The resulting organic solution was dried and concentrated yielding a dark purple solid. The product was then purified on a Et_3N treated silica column using a gradient eluent system (first 5% acetonitrile in dichloromethane until yellow BpyPtCl$_2$ had eluted, then 100% acetone). The product forms strong interactions with the silica so 100% methanol is used to elute the remaining product. Then, the product containing fractions (identified via TLC) were combined, concentrated, and dried in a vacuum descicator yielding 138mg of dark purple solid (84% yield). ^{1}H NMR (400 MHz, DMSO-d_6) δ 9.09 (d, *J* = 6.00 Hz, 2H), 9.05 (d, *J* = 6.25 Hz, 2H), 8.60 (d, *J* = 1.88 Hz, 2H), 8.59 (d, *J* = 1.63 Hz, 2H), 7.93 (dd, *J* = 6.28, 1.90 Hz, 2H), 7.79 (dd, *J* = 6.25, 2.00 Hz, 2H), 7.48 (s, 4H), 6.74 (d, *J* = 2.13 Hz, 2H), 6.58 (d, *J* = 2.38 Hz, 2H), 1.52 (s, 18H), 1.45 (s, 18H), 1.45 (s, 18H). ^{13}C NMR (101 MHz, DMSO-d_6) δ 171.99, 164.61, 163.38, 163.07, 162.92, 161.40, 155.55, 148.28, 147.57, 139.08, 134.36, 128.66, 126.73, 125.83, 124.90, 124.38, 121.55, 111.41, 45.46, 40.43, 29.91, 29.78, 29.76, 8.57. HRMS (ESI) m/z: [M+H]$^+$ Calcd for $C_{62}H_{74}N_4O_4Pt_2$ 1329.50559; Found 1329.50339.

***m*-Ph[(CAT)Pt(bpy)]$_2$. *m*-Ph[(CATH$_2$]$_2$** (34 mg, 0.084 mmol) and 4,4'-di-tert-butyl-2,2'-dipyridyl platinum dichloride (bpyPtCl$_2$)[30] (81 mg, 0.15 mmol) were placed in an oven dried Schlenk flask and purged with argon. Then degassed dimethyl sulfoxide (2 mL) was added to the reaction. Potassium carbonate (42 mg, 0.30mmol) was then added to the reaction and the solution was stirred in an argon atmosphere at room temperature for 46h. The resulting dark purple solution was then dripped into a stirring solution of saturated sodium chloride (100 mL) resulting in the precipitation of a dark a purple solid. This precipitate was collected via vacuum filtration and dissolved in ethyl acetate and dichloromethane. The resulting organic solution was dried and concentrated yielding a dark purple solid. The product was then purified on a Et_3N treated silica column using a gradient eluent system (first 5% acetonitrile in dichloromethane until yellow BpyPtCl$_2$ had eluted, then 50% acetonitrile in dichloromethane, then 100% methanol to elute the remaining product). Then, the product containing fractions (identified via thin layer chromatography) were combined and concentrated, yielding 15 mg of dark purple solid (15% yield). ^{1}H NMR (400 MHz, DMSO-d_6) δ 9.10 (d, *J* = 6.13 Hz, 2H), 9.06 (d, *J* = 6.00 Hz, 2H), 8.61 (d, *J* = 1.75 Hz, 2H), 8.60 (d, *J* = 2.00 Hz, 2H), 7.93 (dd, *J* = 6.13, 2.00 Hz, 2H), 7.78 (dd, *J* = 6.13, 2.00 Hz, 2H), 7.57 (s, 1H), 7.30 (s, 3H), 6.75 (d, *J* = 2.13 Hz, 2H), 6.59 (d, *J* = 2.13 Hz, 2H), 1.52 (s, 18H), 1.45 (s, 18H), 1.45 (s, 18H). ^{13}C NMR (101 MHz, DMSO) δ 163.41, 163.06, 162.93, 161.58, 155.56, 148.34, 147.58, 142.74, 134.36, 128.73, 127.39, 124.91, 124.35, 123.43, 122.74, 121.46, 121.37, 111.79, 110.76, 35.98, 35.92, 34.15, 30.70, 29.92, 29.76. HRMS (ESI) m/z: [M+H]$^+$ Calcd for $C_{62}H_{74}N_4O_4Pt_2$ 1329.50559; Found 1329.50588.

Author Contributions

D.A.S., RS, and M.L.K. all contributed to writing this manuscript. D.A.S. and M.L.K. developed the research project and R.S. synthesized and characterized all molecules and complexes.

Conflicts of interest

There are no conflicts to declare.

Acknowledgements

D. A. Shultz and M. L. Kirk acknowledge financial support from DOE (DE-SC0020199). We thank Prof. Michael Therien for use of and assistance with transient absorption spectroscopy.

Notes and references

1. S. D. Cummings and R. Eisenberg, *J. Am. Chem. Soc.*, 1996, **118**, 1949-1960.
2. S. D. Cummings and R. Eisenberg, in *Progress in Inorganic Chemistry: Synthesis, Properties, and Applications*, ed. E. I. Stiefel, 2004, vol. 52, pp. 315-367.
3. M. Hissler, J. E. McGarrah, W. B. Connick, D. K. Geiger, S. D. Cummings and R. Eisenberg, *Coord. Chem. Rev.*, 2000, **208**, 115-137.
4. W. Paw, S. D. Cummings, M. A. Mansour, W. B. Connick, D. K. Geiger and R. Eisenberg, *Coord. Chem. Rev.*, 1998, **171**, 125-150.
5. J. A. Zuleta, C. A. Chesta and R. Eisenberg, *J. Am. Chem. Soc.*, 1989, **111**, 8916-8917.
6. J. A. Zuleta, M. S. Burberry and R. Eisenberg, *Coord. Chem. Rev.*, 1990, **97**, 47-64.
7. J. A. Zuleta, J. M. Bevilacqua and R. Eisenberg, *Coord. Chem. Rev.*, 1991, **111**, 237-248.
8. J. A. Zuleta, J. M. Bevilacqua, D. M. Proserpio, P. D. Harvey and R. Eisenberg, *Inorg. Chem.*, 1992, **31**, 2396-2404.
9. C. J. Adams, N. Fey, M. Parfitt, S. J. A. Pope and J. A. Weinstein, *Dalton Trans.*, 2007, DOI: 10.1039/b709252k, 4446-4456.
10. J. Yang, D. Kersi, C. P. Richers, L. J. Giles, R. Dangi, B. W. Stein, C. Feng, C. R. Tichnell, D. A. Shultz and M. L. Kirk, *Inorg. Chem.*, 2018, **57**, 13470–13476.
11. J. Yang, D. K. Kersi, L. J. Giles, B. W. Stein, C. Feng, C. R. Tichnell, D. A. Shultz and M. L. Kirk, *Inorg. Chem.*, 2014, **53**, 4791–4793.
12. W. W. Kramer, L. A. Cameron, R. A. Zarkesh, J. W. Ziller and A. F. Heyduk, *Inorg. Chem.*, 2014, **53**, 8825-8837.
13. N. M. Shavaleev, E. S. Davies, H. Adams, J. Best and J. A. Weinstein, *Inorg. Chem.*, 2008, **47**, 1532–1547.
14. P. A. Scattergood, P. Jesus, H. Adams, M. Delor, I. V. Sazanovich, H. D. Burrows, C. Serpa and J. A. Weinstein, *Dalt. Trans.*, 2015, **44**, 11705-11716.
15. M. L. Kirk, D. A. Shultz, P. Hewitt and A. van der Est, *J. Am. Chem. Soc.*, 2022, **144**, 12781-12788.
16. M. L. Kirk, D. A. Shultz, P. Hewitt and A. van der Est, *J. Phys. Chem. Lett.*, 2022, **13**, 872-878.
17. M. L. Kirk, D. A. Shultz, P. Hewitt, D. E. Stasiw, J. Chen and A. van der Est, *Chem. Sci.*, 2021, **12**, 13704-13710.

18. M. L. Kirk, D. A. Shultz, J. Chen, P. Hewitt, D. Daley, S. Paudel and A. van Der Est, *J. Am. Chem. Soc.*, 2021, **143**, 10519-10523.
19. M. R. Wasielewski, M. D. E. Forbes, N. L. Frank, K. Kowalski, G. D. Scholes, J. Yuen-Zhou, M. A. Baldo, D. E. Freedman, R. H. Goldsmith, T. Goodson, M. L. Kirk, J. K. McCusker, J. P. Ogilvie, D. A. Shultz, S. Stoll and K. B. Whaley, *Nat. Rev. Chem.*, 2020, **4**, 490-504.
20. C. R. Tichnell, D. R. Daley, B. W. Stein, D. A. Shultz, M. L. Kirk and E. O. Danilov, *J. Am. Chem. Soc.*, 2019, **141**, 3986-3992.
21. P. Hewitt, D. A. Shultz and M. L. Kirk, *J. Org. Chem.*, 2021, **86**, 15577–15587.
22. B. Stein, C. Tichnell, J. Chen, D. A. Shultz and M. L. Kirk, *J. Am. Chem. Soc.*, 2018, **140**, 2221-2228.
23. J. Best, I. V. Sazanovich, H. Adams, R. D. Bennett, E. S. Davies, A. J. H. M. Meijer, M. Towrie, S. A. Tikhomirov, O. V. Bouganov, M. D. Ward and J. A. Weinstein, *Inorg. Chem.*, 2010, **49**, 10041.
24. S. G. Telfer, T. M. McLean and M. R. Waterland, *Dalt. Trans.*, 2011, **40**, 3097-3108.
25. A. Bencini, C. A. Daul, A. Dei, F. Mariotti, H. Lee, D. A. Shultz and L. Sorace, *Inorg. Chem.*, 2001, **40**, 1582-1590.
26. D. A. Shultz, H. Lee and K. P. Gwaltney, *J. Org. Chem.*, 1998, **63**, 7584-7585.
27. M. Kasha, H. R. Rawls and M. Ashrafel-Bayoumi, *Pure & Appl. Chem.*, 1965, **11**, 371-392.
28. A. L. Thompson, T.-S. Ahn, K. R. J. Thomas, S. Thayumanavan, T. J. Martınez and C. J. Bardeen, *J. Am. Chem. Soc.*, 2005, **127**, 6348-16349.
29. N. J. Turro, V. Ramamurthy and J. C. Sciano, *Modern Molecular Photochemistry of Organic Molecules*, University Science Books, 2010.
30. J. Vicente, P. Gonzalez-Herrero, M. Perez-Cadenas, P. G. Jones and D. Bautista, *Inorg. Chem.*, 2007, **46**, 4718-4732.